Identification of Potential *Candida albicans* Inhibitors Through Pharmacophore Modeling and Virtual Screening

ABSTRACT

Fungal infections have increased significantly in recent years and represent a major threat to human health. A large number of these infections are caused by the opportunistic pathogen Candida albicans. Lanosterol 14-alpha demethylase (CYP51), a critical enzyme in the cytochrome P450 family, is a well-established target for antifungal drugs. However, increasing resistance to current antifungal treatments has created an urgent need for the development of new therapies with improved biological activity.

In this study, we focused on Candida albicans and used the target protein (PDB code: 1EA1) to perform an in silico analysis of a series of benzimidazole derivatives. The aim was to identify novel chemotherapeutic agents with potential antifungal activity. To discover new Candida albicans inhibitors, pharmacophore models based on the molecular structure of rhodanine derivatives were generated and validated using various methods. A virtual screening of the Enamine database was performed based on the combinatorial pharmacophore model. Compounds selected after virtual screening were subjected to molecular docking protocols (HTVS, SP, XP and IFD).

A total of 26 new active compounds were identified and their absorption, distribution, metabolism and excretion (ADME) properties were calculated. These results suggest that the identified compounds could serve as promising chemical starting points for further structural optimisation in the development of Candida albicans inhibitors.

Keywords: Benzimidazole, candida albicans, pharmacophore,virtual screening, molecular docking.

1.INTRODUCTION

Recently, fungal infections have significantly increased and have become serious threats to human health. Fungal infections can be classified into two types : superficial and systemic.[1].

The increased incidence of candidiasis and the impressive rate of drug resistance have prompted researchers to develop new and more effective antifungal agents.

Opportunistic candidiasis, mainly candida albicans, is responsible for this complicated fungal infection with 50 to 90% of human candidiasis [2, 3].

On the other hand, systemic infections are very dangerous, especially for immunocompromised people, including AIDS patients. [4, 5].

Many fungal infections such as neutropenia, endocarditis, endophthalmos, meningitis, intra-abdominal candidiasis, osteomyelitis, and fungal arthritis are caused by the opportunistic pathogen Candida albicans [6]. Lanosterol 14-alpha-demethylase (CYP51), which belongs to the cytochrome P450 family, is a well-known and common antifungal target. [7, 8].

In clinical practice, there are limited antifungal agents that can be used for life-threatening fungal infections. These drugs fall into 5 main classes: azoles, allylamines, polyenes, fluoropyrimidines and thiocarbamates [9].

Among them, azoles are the most widely used antifungal agents due to their high therapeutic index. Azoles are a large and relatively new group of synthetic compounds, of which imidazoles and triazoles are two clinically useful families used in the treatment of systemic fungal infections as well as in agriculture [10, 11, 5]. In this research, the combination of pharmacophore modelling, virtual screening and molecular docking was performed on a series of benzimidazole-derived molecules synthesised by Zon et al[12, 13] for the discovery of potential new inhibitors of candida albicans.

2. Materials and methods
2.1 Selection of biological dataset

A data set of 74 benzimidazole derivatives with their antifungal activityQMI (μg) as inhibitors of fungal infection was obtained from the work of Zon et al.[13, 12]. All molecular structures and activity data utilized for pharmacophore modeling, virtual screening, and molecular docking are presented in Table 2. In these studies, the inhibitory activities (QMI values in M) for each compound were converted to their negative logarithmic form (pQMI). All compounds share a similar structure and were evaluated using the same bioassay method.

2.2 Ligand preparation

The 3D structures of the ligands were generated using the construction panel in Maestro and optimized with the LigPrep module [14]. Partial atomic charges were assigned, and possible ionization states were generated at a pH of 7.0 ± 2.0. The OPLS_2005 force field was employed to optimize the production of the lowest energy ligand conformer[15]. Energy minimization was performed for each ligand until it reached a root mean square deviation threshold of 0.01 Å.

2.3 Pharmacophore model generation

Schrödinger's Phase module for ligand-based drug design was used to develop pharmacophore hypotheses [16]. The chemical characteristics of all ligands were defined by six pharmacophore features: hydrogen bond acceptor (A), hydrogen bond donor (D), hydrophobic group (H), negatively charged group (N), positively charged group (P), and aromatic ring (R). An active analogue approach was applied to identify common pharmacophore hypotheses, where common pharmacophores were selected from the conformations of the active ligand set using a hierarchical partitioning technique that groups similar pharmacophores based on their inter-site distances [17]The identified pharmacophores were subsequently recorded and categorized. A scoring process was conducted to determine the most promising candidate hypothesis, which resulted in an overall ranking of all the hypotheses. The

scoring algorithm took into account factors such as site point and vector alignment, volume overlap, selectivity, the number of paired ligands, relative conformational energy, and biological activity.[17].

2.4 Pharmacophore Validation

Validating a pharmacophore model is a crucial initial step to ensure its accuracy and specificity in selecting active molecules, while also guiding the virtual screening of ligands from a database. In this study, a set of 218 decoy molecules from the Directory of Useful Decoys(http://dude.docking.org/) [18, 19]supplemented with 20 active molecules, was used. These 20 *Candida albicans* inhibitors were not included in the construction of the pharmacophore models. Prior to validation, the preprocessing of both the active and decoy datasets was carried out using the LigPrep module. All possible ionizable states and tautomeric forms at a pH range of 7.0 ± 2.0 were generated using this module[14]. For each compound, up to 32 conformers were generated by default, and low-energy stereoisomers with correct chirality were selected for further analysis. The Phase module's hypothesis validation tool[20]was employed for this process. This tool uses the hypothesis file along with the decoy and active datasets to calculate performance parameters. Several statistical parameters, including Enrichment Factors (EF), Robust Initial Improvement (RIE), Boltzmann Enhanced Discrimination of Receiver Operating Characteristic (BEDROC), Area Under the Accumulation Curve (AUC), and Receiver Operating Characteristics (ROC), were computed to validate the hypothesis[21].

2.5 Guner – Henry score validation

The Güner-Henry (GH) scoring method is employed to quantify the selectivity of a pharmacophore model and assess its effectiveness in similarity-based searching. This scoring method identifies the active molecules within a dataset comprising both known active and inactive compounds. The score ranges from 0 to 1, with 0 representing a null model and 1 indicating an ideal model. A score greater than 0.7 is typically expected[22]. The formulas used to calculate the GH score are provided below:

$$GH = \left(\frac{H_a(3A + H_t)}{4H_t A}\right)\left(1 - \frac{H_t - H_a}{D - A}\right)$$

$$\%A = \frac{H_a}{A} \, X \, 100 \; ; \%Y = \frac{H_a}{H_t} \, X \, 100 \; ; EF = \frac{H_a/H_t}{A/D}$$

In the GH scoring method, Ha represents the number of active compounds in the hits list (true positives), A is the total number of active compounds in the database, Ht is the total number of hits retrieved, and D is the total number of compounds in the database. %A indicates the percentage of known active compounds obtained from the database, while %Y refers to the percentage of known active compounds in the hits list. EF stands for the enrichment factor, which quantifies the concentration of actives retrieved by the model compared to random screening without using a pharmacophore approach.The Güner-Henry score is considered an important metric, as it accounts for both the percentage yield of actives in the database (%Y) and the percentage ratio of actives in the hits list (%A).

2.6 High throughput virtual screening and molecular docking

The molecules obtained after pharmacophore screening were subjected to filtering through High Throughput Virtual Screening (HTVS), followed by Glide docking using Standard Precision (SP) and Extra Precision (XP) methods at the crystal structure binding sites with Glide. The co-crystallized ligand was centered for grid generation using Glide's grid generation tools. Post-docking minimization was carried out using MM-GBSA (Molecular Mechanics energies combined with Generalized Born and Surface Area) to optimize the geometries of the retrieved molecules. The top 10% of the molecules from each step were selected for further analysis. Finally, all non-peptide molecules (since peptide compounds are orally degradable) were processed using the Glide XP molecular docking system, employing the 1EA1 crystal structure to evaluate the docking scores of the resulting molecules after screening.

2.7 Induced fit docking

An induced fit docking (IFD) method[23], where the receptor is flexible during the docking process, was employed in this study. The energy minimization of the protein structure was carried out using the OPLS_2005 force field. The prepared molecules were docked to the rigid protein using Glide with default parameters. Energy minimization was applied to the crystal structure of PDB code: 1EA1. XP

molecular docking was used for the initial docking, and 25 ligand poses were retained for the refinement of the protein structure. Schrödinger's 2017-4 Prime module was then used to refine residues within 5.0 Å of the ligand poses, leading to the development of induced fit protein-ligand complexes. After these refinements[24], the ranking of each of the 26 complexes was performed based on Prime energy. Complexes with an energy below -25 kcal/mol were re-docked for the final step of scoring. Each ligand was docked into the refined low-energy receptor structures developed during the refinement step. The binding affinity of each complex was estimated using the docking score. The lowest negative docking and IFD scores were considered to represent the most favorable binding conditions with the active site of 1EA1.

2.8 ADME prediction

The QikProp tool from Schrödinger[25]was used to predict the drug-like properties of the ten best hits by evaluating their ADME (Absorption, Distribution, Metabolism, and Excretion) profile. During this process, the Lipinski rule of five was applied, and various descriptors, such as QPlogHERG, QPPCaco, QPlogBB, and the percentage of human oral absorption, were calculated.

3. Results and discussions

3 .1 Generation of pharmacophore models

We developed ligand-based pharmacophore models that identified the pharmacophore points required to inhibit the biological activity of candida albican. The molecules in the dataset were divided into active, inactive and moderately active molecules. Molecules with a pQMI (pQMI= -log(QMI)) greater than 8 were considered active and those with a pQMI less than 7.5 were considered inactive, while compounds with a pQMI between the threshold values were considered moderately active.
Pharmacophore models containing 4 to 5 sites were generated using four features: hydrogen bond acceptor (A), hydrogen bond donor (D), hydrophobic (H) and aromatic ring (R). The quality of the pharmacophore models was evaluated using site score, vector score, volume score, survival score and BEDROC score[26] . Among the generated pharmacophore models, the eight best models (Table 1) were selected on the basis of the survival score parameter. A good pharmacophoric model is characterised by a high value of the parameters Survival score[26] . The models obtained have a survival score between 4.483 and 5.324. (Table 1) The ADRRR_1 model has the highest survival score of 5.324. This model includes a hydrogen bond acceptor (A), a hydrogen bond donor (D) and three aromatic rings (R).

3.2 Validation of the pharmacophore : the Decoy method

The constructed pharmacophore models were validated using a set of parameters (Table 3) calculated from a database containing 218 decoy molecules, enriched with 20 candida albicans inhibitors that were not used in the construction of the pharmacophore models. The database was screened with the pharmacophores obtained using the phase software screening tool. For the different pharmacophoric models, the enrichment factor at 1% is between 5.95- 11.90 and the GH (goodness of hit) parameter is between 0.78 and 1. These results indicate that the different pharmacophores generated show a high selectivity with respect to the active molecules.

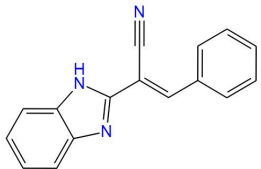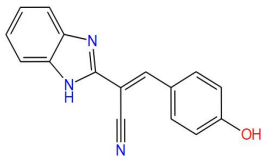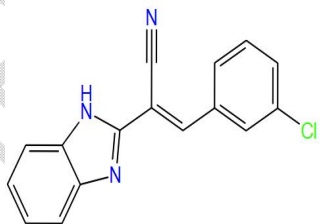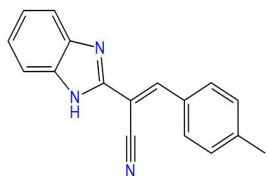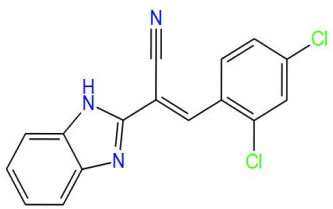**Table 1.the obtained pharmacophore models and Scoring parameters**
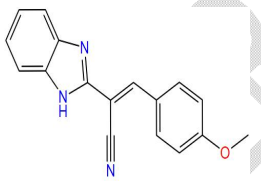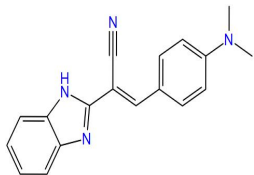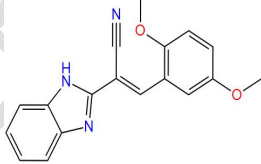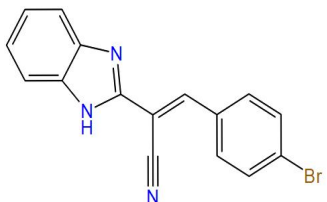
Model	Vector Score	Volume Score	Survival Score	Site Score	Selectivity Score	Adjusted Score	BEDROC Score	PHS[a]
ARRR_1	0.938	0.760	5.224	0.817	1.277	5.224	0.754	1.068
ARRR_2	0.881	0.619	4.895	0.586	1.265	4.895	0.523	0.817
HRRR_1	0.784	0.579	4.953	0.502	1.531	4.953	0.465	0.763
ADRR_1	0.923	0.726	5.198	0.804	1.201	5.198	0.716	1.028
ADRR_2	0.991	0.872	4.883	0.918	1.199	4.883	0.520	0.813
ADRRR_2	0.982	0.872	5.285	0.900	1.627	5.285	0.535	0.852
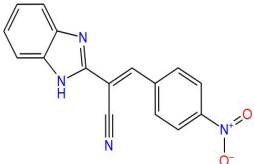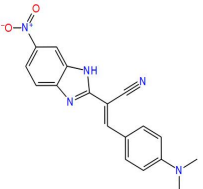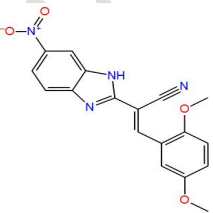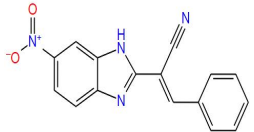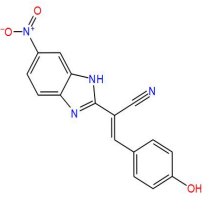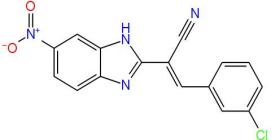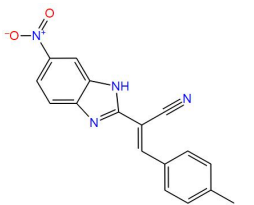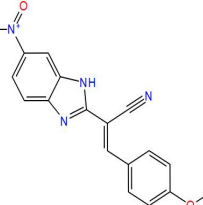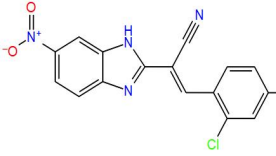
ADRRR_1	0.982	0.873	5.324	0.899	1.668	5.324	0.526	0.846
AADRR_2	0.982	0.873	5.076	0.892	1.426	5.076	0.533	0.838
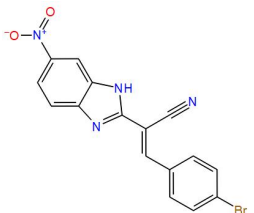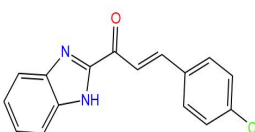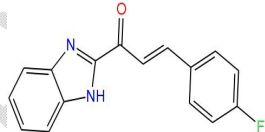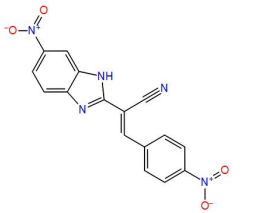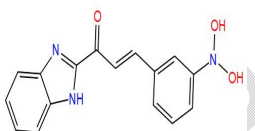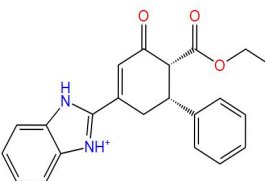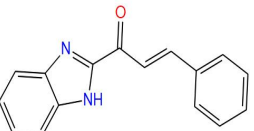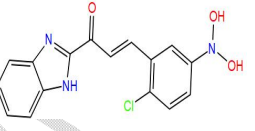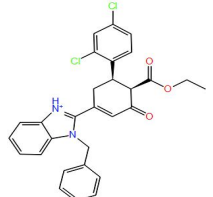
a :Phase hypo score
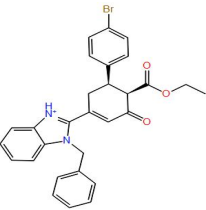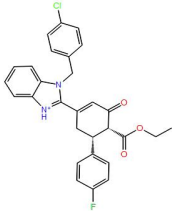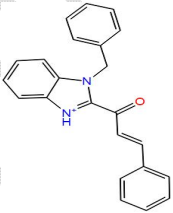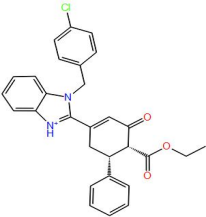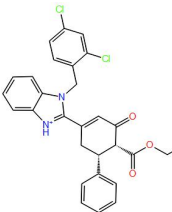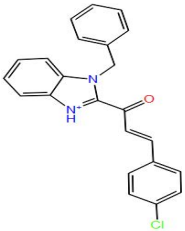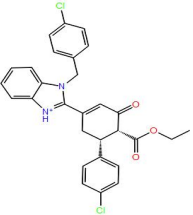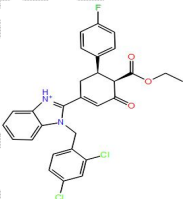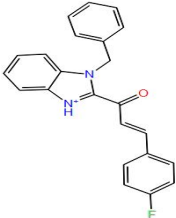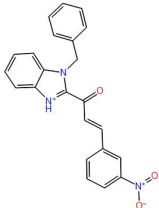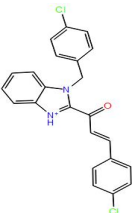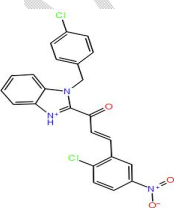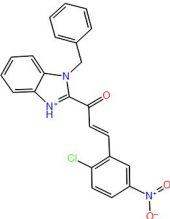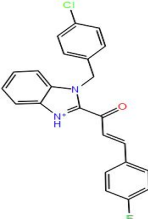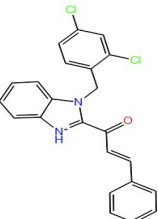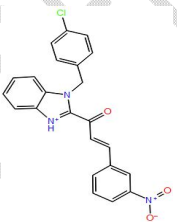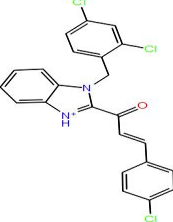
Table2.Structure of benzimidazoles and their biological activities pQMI

Ligands	Structure	Activity	Ligands	Structure	Activity	Ligands	Structure	Activity
A1		7.3897	A4		7.4171	A7		7.4467
A2		7.4138	A5		7.439	A8		7.4972
A3		7.4599	A6		7.485	A9		7.5108

Ligands	Structure	Activity	Ligands	Structure	Activity	Ligands	Structure	Activity
A10		7.4628	A13		7.523	A16		7.5445
A11		7.4628	A14		7.486	A17		8.4146
A12		7.4833	A15		7.505	A18		9.3512

Ligands	Structure	Activity	Ligands	Structure	Activity	Ligands	Structure	Activity
A19		9.3631	A22		7.451	A25		8.6295
A20		7.5254	A23		7.467	B26		7.5568
A21		8.2980	A24		7.515	B27		7.7155

Ligands	Structure	Activity	Ligands	Structure	Activity	Ligands	Structure	Activity
B28		7.7238	B31		7.7015	B34		7.5294
B29		7.6857	B32		7.7155	B35		7.5715
B30		7.7155	B33		7.7303	B36		7.5519

Ligands	Structure	Activity	Ligands	Structure	Activity	Ligands	Structure	Activity
B37		7.5837	B40		7.6099	B43		7.9564
B38		7.6210	B41		7.5920	B44		7.6099
B39		7.5715	B42		7.6210	B45		7.6452

Ligands	Structure	Activity	Ligands	Structure	Activity	Ligands	Structure	Activity
B46		7.6287	C49		7.4171	C52		7.4460
B47		7.6554	C50		7.4644	C53		7.4861
B48		7.6873	C51		7.4709	C54		7.4861
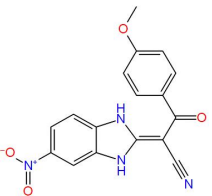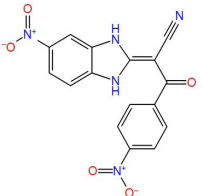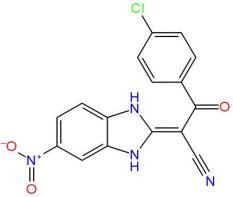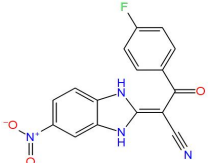
Ligands	Structure	Activity	Ligands	Structure	Activity	Ligands	Structure	Activity
C55		7.5267	C58		8.7501			
C56		7.5324						
C57		7.5109						

Table3. Validation of pharmacophore models by the DECOY method

Model	D	A	Ht	Ha	%Y	%A	FN	FP	EF1	BEDROC	ROC	AUC	RIE	GH
ARRR_1	238	20	27	20	74.07	100	0	7	11.90	1.00	0.97	0.93	8.49	0.7797
ARRR_2	238	20	25	20	80	100	0	5	11.90	1.00	0.98	0.94	8.56	0.8305
HRRR_1	238	20	27	20	74.074	100	0	7	5.95	0.75	0.97	0.93	7.11	0.7797
ADRR_1	238	20	21	20	95.24	100	0	1	11.90	1.00	1.00	0.95	9.38	0.9599
ADRRR_2	238	20	21	20	95.24	100	0	1	11.90	1.00	0.99	0.95	9.30	0.9599
AADRRR_1	238	20	21	20	95.2381	100	0	1	11.90	1.00	1.00	0.95	9.38	0.9599
AADRR_2	238	20	21	20	95.2381	100	0	1	11.90	1.00	0.99	0.95	9.30	0.9599
ADRR_2	238	20	20	20	100	100	0	0	11.90	1.00	0.50	0.73	6.76	1.0000

a) ARRR_1
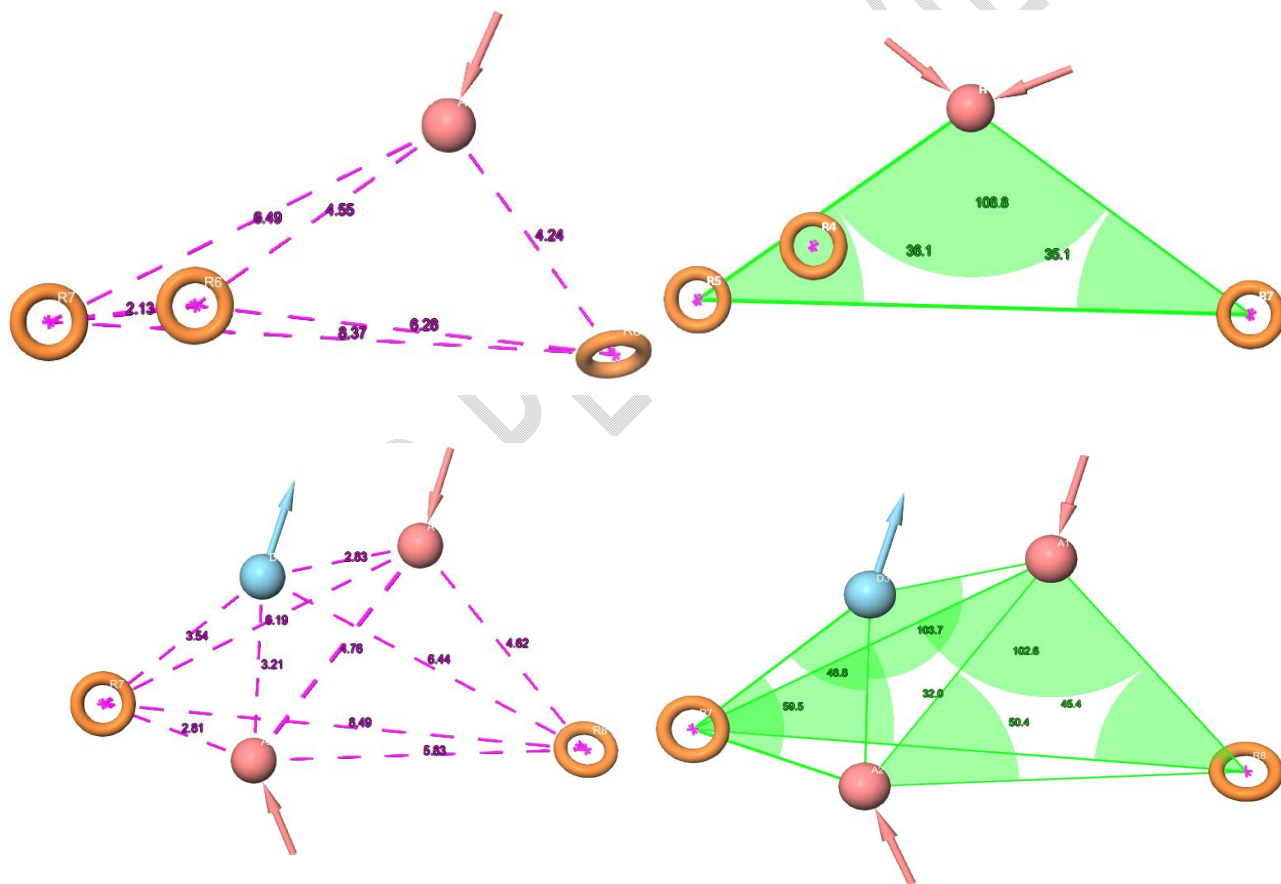
b) AADRR_2

Fig. 1. 3D representation of the pharmacophore models a) ARRR_1 b) AADRR_2 with distances and angles between the different pharmacophore sites.

These results indicate that the different pharmacophores generated show a high selectivity towards the active molecules. The different hits obtained during the validation were also statistically analysed using the ROC curve, which is a graphical representation of the relationship between the sensitivity and specificity of the virtual screening process.The ROC curve represents the fraction of VPs (among the active) versus theVNs(among the inactive) obtained during the screening of the database.The

parameter characterising the ROC curve is between 0 and 1. Truchon and Baylay [27]considered an ROC value of 0.7 as a desirable performance value. In the present study, the ROC parameters of the different pharmacophore models ranging from 0.97 to 1 indicate that the different models are able to distinguish active from inactive molecules in the virtual screening process (Figure 2).
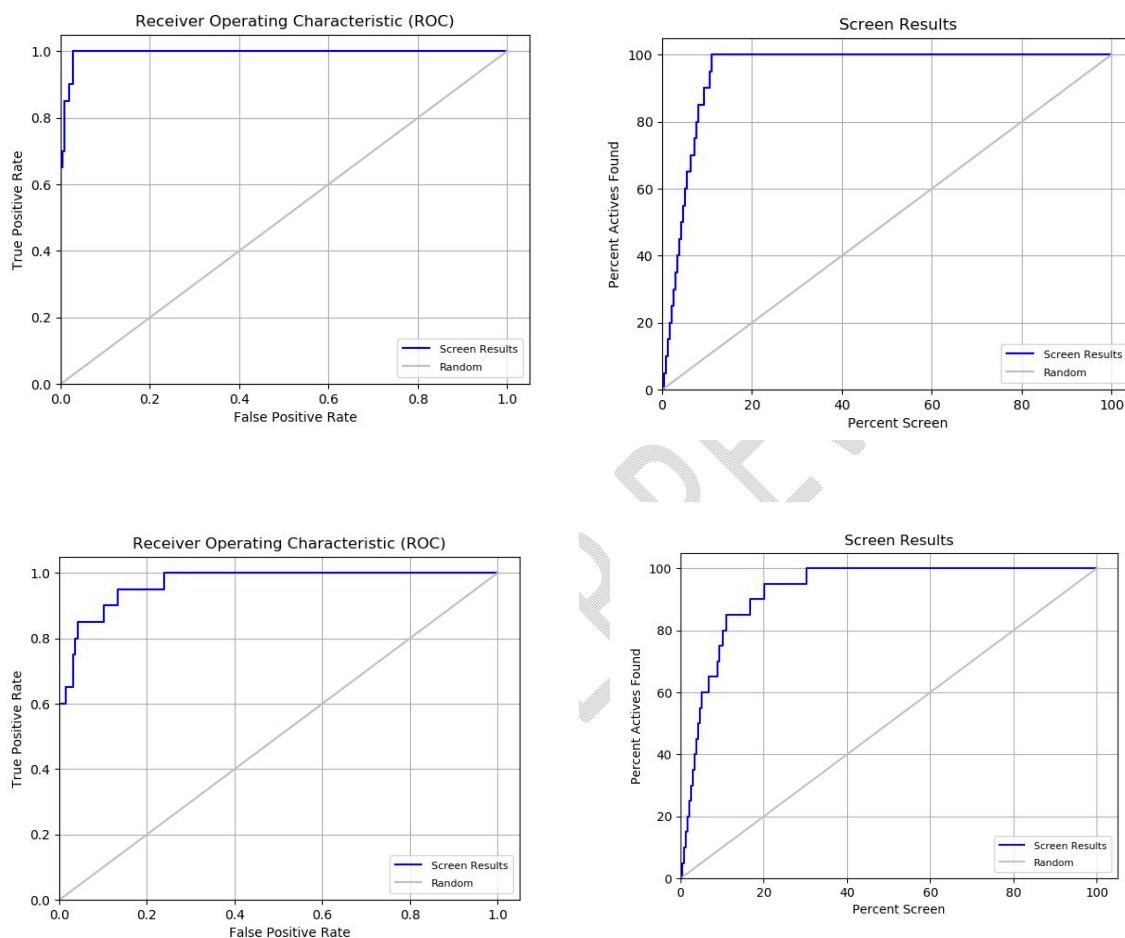
Fig. 2.ROC curve of the pharmacophore models AADRR_2 , ARRR_1

The AUC metric of the ROC curve was also considered to test the performance of the different pharmacophorical models. The pharmacophore models obtained have a significant AUC between 0.73-0.95 (Table 3). These values of the AUC metric highlight the reliability of the different pharmacophore models in identifying new compounds in a virtual screening experiment. Consequently, all the parameters calculated for the assessment of the quality of the pharmacophores suggest that these pharmacophoric models have a high predictive power in the identification of active compounds in a chemical library thus providing a starting point for the identification of new inhibitors of *candida albicans*.

3.3 Virtual screening of the Enamine chemical library

Virtual screening based on ligands from a database of molecules (chemical library) is a widely used technique in the drug design process for the identification of new hits [28]**.** Screening a database using pharmacophore models facilitates the screening of millions of multi-conformational compounds at once. The validated pharmacophore models were used for virtual screening of the phase.dtb database created from the "sdf" format files from the ENAMINE database.This database contains 535326, Molecules approximately 13383150 conformations. The screening of the database using

pharmacophore models as "three-dimensional queries" yielded 78,000 molecules which were then used in the VSW (Virtual Screening Workflow) protocol of the Schrodinger suite. The VSW protocol is a multi-step virtual docking screening process of the schrodinger package, which includes different steps with increasing molecular docking accuracies. This protocol was used to screen by molecular docking the compounds obtained after screening the database by the different pharmacophore models.

Table 4.Hits obtained after virtual screening using pharmacophore models and molecular docking

Title	Vector Score	Matched Ligand Sites	Hypo ID	Align Score	Phase Screen Score	Fitness	Volume Score
Z1804044680	0.837	A(1) R(11) R(10) R(12)	ARRR_1	0.452	2.025	2.025	0.564
PV-001850708261	0.842	A(4) R(11) R(10) R(12)	ARRR_2	0.440	2.094	2.094	0.618
Z2283404606	0.916	H(7) R(9) R(8) R(10)	HRRR_1	0.381	2.041	2.041	0.442
Z1651668373	0.816	H(5) R(6) R(8) R(7)	HRRR_1	0.401	1.924	1.924	0.443
PV-001935350830	0.970	A(1) R(11) R(10) R(9)	ARRR_2	0.505	2.240	2.240	0.690
PV-001831793679	0.893	A(3) R(11) R(10) R(12)	ARRR_2	0.330	2.196	2.196	0.578
PV-001862316134	0.784	A(2) R(11) R(12) R(10)	ARRR_1	0.377	1.996	1.996	0.527
PV-001924736320	0.927	A(2) R(6) R(9) R(8)	ARRR_2	0.292	2.395	2.395	0.711
Z1545254023	0.971	H(6) R(8) R(7) R(9)	HRRR_1	0.446	2.128	2.128	0.529
PV-001925585102	0.934	A(1) R(8) R(7) R(9)	ARRR_1	0.476	2.177	2.177	0.641
Z2141883735	0.954	H(7) R(10) R(9) R(11)	HRRR_1	0.429	2.004	2.004	0.407
PV-001921223059	0.983	H(7) R(9) R(10) R(8)	HRRR_1	0.421	2.035	2.035	0.402
Z2770976320	0.877	A(3) R(9) R(10) R(8)	ARRR_2	0.438	2.162	2.162	0.650
Z2903058602	0.931	A(5) R(11) R(12) R(10)	ARRR_2	0.478	2.228	2.228	0.695
Z2193901479	0.766	A(2) R(12) R(11) R(13)	ARRR_2	0.346	2.085	2.085	0.607
Z2218766564	0.756	A(2) R(9) R(11) R(10)	ARRR_2	0.282	2.053	2.053	0.532
Z2903057141	0.978	A(2) R(9) R(11) R(12)	ARRR_1	0.966	1.902	1.902	0.728
PV-000817165047	0.868	A(1) R(8) R(7) R(9)	ARRR_1	0.331	2.137	2.137	0.545
Z2095183789	0.926	H(8) R(10) R(9) R(11)	HRRR_1	0.526	1.904	1.904	0.417
Z3188961853	0.843	A(2) R(8) R(7) R(9)	ARRR_1	0.495	1.919	1.919	0.489
Z2923423811	0.913	A(2) R(10) R(9) R(11)	ARRR_1	0.492	2.079	2.079	0.576
PV-002587460686	0.843	A(2) A(1) D(6) R(12) R(14)	AADRR_2	0.570	2.026	2.026	0.658
PV-001936869335	0.855	A(2) R(13) R(12) R(11)	ARRR_1	0.405	2.090	2.090	0.572
Z1498805014	0.911	A(2) R(11) R(10) R(12)	ARRR_1	0.711	1.858	1.858	0.540
Z1849714935	0.935	D(3) R(7) R(9) R(8)	DRRR_2	0.343	2.157	2.157	0.508
Z1753455598	0.840	D(7) R(10) R(12) R(11)	DRRR_2	0.537	1.876	1.876	0.484

All ligands were initially screened in high-throughput virtual screening (HTVS) mode and the top 10% of compounds were docked with Glide SP. Subsequently, the top 10% of compounds, but retaining only good score states, were processed by docking with Glide XP. At this stage, the default number of poses per compound state was increased to 5. Finally, 10% of the best compounds retaining only the best scoring states were obtained as output.

Sequential virtual screening including HTVS, SP and XP protocols allowed us to select a total of 2908 molecules which were then used for a Prime MM-GBSA analysis. After the Prime MM-GBSA analysis we selected molecules with energy lower than that of the co-crystallised ligand Fluconazole (ΔG_bind=-25 kcal/mol) . To take into account the flexibility of the protein. The resulting set of molecules was subjected to the IFD protocol. The sequential virtual screening including HTVS, SP, XP, MM-GBSA prime and IFD protocols allowed us to select a total of 26 hits. Table 4 shows the 26 hits with their fitness scores and the pharmacophore models that were used to retrieve them during the virtual screening. The values of the fitness score parameter for the keys range from 1.858 to

2.395. The lead PV-001924736320 retrieved by the pharmacophoric model ARRR_2 tops the list with a fitness score of 2.395 (Figure 3).
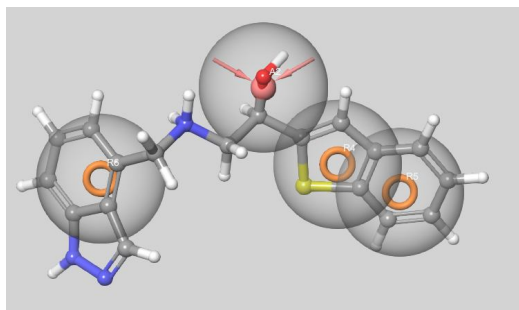

Fig.2.Lead PV-001924736320 aligned to pharmacophore model ARRR_2

3.4 HTVS SP and XP analysis of hits

Table5.HTVS, SP, XP docking parameters of the obtained leads (in kcal/mol)

Touches	HTVS DOCKING			SP DOCKING			XP DOCKING		
	DOCKING SCORE	GLIDE ENERGY	GLIDE EMODEL	DOCKING SCORE	GLIDE ENERGY	GLIDE EMODEL	DOCKING SCORE	GLIDE ENERGY	GLIDE EMODEL
Z1804044680	-8.923	-47.714	-67.736	-11.140	-58.983	-93.243	-12.161	-53.130	-86.339
PV-001850708261	-9.456	-46.775	-73.427	-9.677	-54.878	-79.107	-10.841	-48.680	-84.414
Z2283404606	-9.319	-48.942	-68.945	-10.032	-51.520	-78.635	-10.885	-50.793	-87.113
Z1651668373	-5.962	-22.518	-17.878	-9.837	-52.321	-78.018	-10.970	-52.134	-88.625
PV-001935350830	-8.786	-41.495	-34.354	-10.757	-56.845	-91.132	-12.019	-56.954	-90.977
PV-001831793679	-9.122	-45.311	-64.560	-7.099	-53.391	-67.379	-10.848	-61.488	-87.027
PV-001862316134	-7.761	-27.803	-17.614	-9.564	-46.508	-64.530	-10.905	-48.342	-60.834
PV-001924736320	-9.551	-30.789	-47.971	-11.242	-56.392	-87.522	-12.041	-54.170	-77.241
Z1545254023	-9.998	-52.021	-81.670	-10.801	-55.752	-88.687	-11.193	-51.986	-83.211
PV-001925585102	-8.824	-32.728	-40.055	-10.086	-47.427	-76.576	-12.424	-52.759	-81.160
Z2141883735	-7.699	-44.061	-55.792	-9.715	-48.526	-71.436	-11.282	-49.391	-74.911
PV-001921223059	-9.157	-31.236	-35.499	-10.489	-53.756	-82.285	-10.824	-52.152	-72.417
Z2770976320	-7.583	-38.050	-48.510	-9.849	-55.290	-73.727	-11.244	-46.239	-79.568
Z2903058602	-10.149	-44.212	-69.213	-10.352	-49.524	-75.927	-11.118	-49.094	-70.696
Z2193901479	-8.672	-41.849	-56.768	-9.482	-52.299	-73.275	-10.843	-46.985	-74.904
Z2218766564	-7.974	-19.684	-16.882	-9.513	-50.575	-77.599	-11.028	-41.036	-71.238
Z2903057141	-9.331	-44.382	-67.541	-10.352	-49.524	-75.927	-10.783	-43.341	-63.562
Z2095183789	-8.378	-36.016	-54.355	-7.405	-46.934	-66.154	-11.793	-62.235	-97.029
Z3188961853	-7.226	-35.821	-34.572	-9.576	-57.547	-82.492	-11.026	-51.761	-72.321
Z2923423811	-8.736	-43.560	-64.569	-9.184	-47.100	-9.184	-11.282	-42.642	-77.004

PV-002587460686	-9.268	-33.162	-38.163	-9.826	-38.487	-9.826	-11.587	-50.164	-60.579
PV-001936869335	-7.811	-47.217	-69.068	-8.890	-56.669	-8.890	-11.303	-55.860	-91.769
Z1498805014	-9.093	-57.122	-92.983	-11.781	-60.787	-11.781	-11.352	-57.472	-102.095
Z1849714935	-8.903	-51.287	-79.031	-10.070	-47.795	-10.070	-11.492	-43.565	-80.866
PV-000817165047	7.972	-40.841	-57.472	-9.782	-56.276	-9.782	-11.410	-57.092	-97.470
Z1753455598	-7.579	-50.350	-68.082	-9.360	-59.338	-9.360	-11.822	-50.956	-88.870
fluconazole	-6.884	-33.107	-37.130	-5.684	-50.727	-67.499	-5.671	-49.571	-74.978

The results by docking glide HTVS, SP and XP of the hits are presented in Table 6. The values of the interaction energy parameters: docking score, glide energy and glide Emodel of the hits obtained by glide XP are between -10.783 and -12.424 kcal/mol; -41.036 and -62.235 kcal/mol; -60.579 and -102.095 kcal/mol respectively. The docking score values of the leads in the different methods HTVS, SP and XP are lower than those of fluconazole. Therefore, these 26 leads have a higher affinity than the reference molecule, which confers a better stability in the active site of the 1EA1 protein target..

3.5 Prime MM-GBSA analysis of hits

The Prime/MM-GBSA method based on the complex obtained after Docking XP was used to calculate the free enthalpy of binding ΔG_bind of the ligands in the active site of the target protein 1EA1 and the results obtained are summarised in Table 7.

The free enthalpy of binding ΔG_{bind} of the leads ranges from -61.03 to -20.45 kcal/mol . According to the energy components of the free enthalpies of binding given in Table 7, the main favourable energetic factors for ligand binding are van der Waals interactions ΔG_{vdW} (ranging from -34.98 to -57.334 kcal/mol), electrostatic or coulomb interactions $\Delta G_{coulomb}$ (ranging from -0.41 to -98.92kcal/mol) and lipophilic interactions ΔG_{lipo} (ranging from -17.417 to -44.71 kcal/mol). Except for the leads Z2903058602 ($\Delta G_{covalent}$ = -0.79kcal/mol) and Z3188961853 ($\Delta G_{covalent}$ =-0.384 kcal/mol) whose covalent interaction energy terms $\Delta G_{covalent}$ contribute favourably to the free enthalpy of bonding, the other leads have a contribution of $\Delta G_{covalent}$ (between 1.69 and 21.77kcal/mol) unfavourable to ligand binding. The solvation interaction energy terms ΔG_{solvGB} (ranging from 38.15 to 124.83 kcal/mol) are significantly unfavourable to ligand binding. Furthermore, apart from the leads Z3188961853, Z2283404606 and Z1753455598, it is evident that the contribution of the hydrogen bonding energy ΔG_{H-bond} (ranging from -2.53 to 1.26 kcal /mol) and the packing energy $\Delta G_{packing}$ (ranging from -0.371 to -8.95kcal /mol) is small in the free enthalpy of binding.Furthermore, the high negative values of ΔG_{vdW} and ΔG_{lipo} indicate the presence of massive hydrophobic interactions between the candida albicans enzyme and the hits obtained.Except for **Z2405188545,**the hits obtained have lower free enthalpies of binding ΔG_{bind} than that of the reference ligand (ΔG_{bind} =-28.178kcal/mol). These results indicate that the hits obtained are suitable for the active site of the *candida albicans* (1EA1) enzyme.

Table 6.Prime MM-GBSA analysis of the hits.

Touches	ΔG_{bind}	$\Delta G_{coulomb}$	$\Delta G_{covalent}$	ΔG_{H-bond}	ΔG_{lipo}	$\Delta G_{packing}$	ΔG_{solvGB}	ΔG_{vdW}
Z1804044680	-48.53	-48.29	7.76	-0.69	-35.37	-4.13	77.91	-45.72
PV-001850708261	-32.054	-21.371	7.578	-0.742	-17.417	-2.568	50.925	-48.459
Z2283404606	-37.162	-34.643	2.090	0.558	-26.944	-0.371	79.064	-56.916
Z1651668373	-58.79	-63.57	9.81	-0.72	-33.44	-5.73	82.36	-47.51
PV-001935350830	-44.46	-16.90	7.72	-1.85	-21.90	-7.04	46.98	-51.48
PV-001831793679	-41.87	-31.00	17.41	-2.03	-44.71	-7.07	72.41	-46.88
PV-001862316134	-28.71	-28.72	9.16	-0.99	-37.22	-7.92	71.96	-34.98

PV-001924736320	-37.51	-53.21	6.23	-0.64	-26.65	-7.50	89.57	-45.31
Z1545254023	-52.01	-70.64	6.45	-1.34	-24.97	-4.81	92.80	-49.51
PV-001925585102	-38.59	-61.77	7.10	-1.28	-26.17	-5.24	95.01	-46.24
Z2141883735	-43.43	-22.43	8.07	-0.73	-31.41	-4.09	50.38	-43.22
PV-001921223059	-51.00	-62.96	8.26	-1.38	-40.26	-4.30	91.29	-41.65
Z2770976320	-45.76	-20.16	11.83	-1.31	-23.00	-6.19	38.15	-45.08
Z2903058602	-32.74	-6.32	-0.79	-0.67	-22.88	-6.87	48.02	-43.23
Z2193901479	-31.67	-12.54	9.65	-0.58	-23.36	-6.13	48.98	-47.68
Z2218766564	-53.99	-61.21	5.94	-0.88	-36.42	-5.79	84.33	-39.97
Z2903057141	-30.42	-12.89	2.72	-0.75	-21.31	-7.29	45.28	-36.18
Z2095183789	-39.62	-35.04	1.69	-1.78	-25.99	-4.53	75.04	-49.01
Z3188961853	-40.144	-44.289	-0.384	0.038	-21.320	-3.717	77.583	-48.056
Z2923423811	-47.50	-26.16	3.04	-1.87	-32.48	-5.04	62.15	-47.14
PV-002587460686	-20.45	-36.38	21.77	-1.81	-33.23	-5.43	78.45	-43.83
PV-001936869335	-41.22	-26.50	3.73	-1.82	-31.59	-5.45	67.73	-47.32
Z1498805014	-61.03	-64.86	8.13	-2.53	-37.16	-4.98	92.79	-52.42
Z1849714935	-53.96	-98.92	7.31	-0.92	-34.44	-5.60	124.83	-46.23
PV-000817165047	-41.93	-64.04	8.50	-0.81	-38.13	-8.95	116.55	-55.05
Z1753455598	-25.725	-0.410	7.476	1.126	-31.513	-4.899	59.830	-57.334
fluconazole	-28.178	-2.588	-1.731	-0.103	-18.113	-8.708	43.713	-40.648

$$\Delta G_{bind} = \Delta G_{coulomb} + \Delta G_{covalent} + \Delta G_{H-bond} + \Delta G_{lipo} + \Delta G_{packing} + \Delta G_{solGB} + \Delta G_{wdw}$$

3.6 IFD analysis of hits

The parameters glide energy, glide Emodel, docking score and IFD score as well as the different types of interactions between the hits obtained and the residues of the active site of the 1EA1 protein are summarised in Table .8.The parameters glide energy, glide Emodel, docking score and IFD score as well as the different types of interactions between the hits obtained and the residues of the active site of the 1EA1 protein are summarised in Table IV.8. The docking score, IFD score, glide Emodel, glide energy parameters of the hits obtained are between -14.041 and -10.229 kcal/mol ; -985.918 and -978.162 kcal/mol ; -112.728 and -75.456 kcal/mol ; -63.187 and -44.602 kcal/mol respectively.

Table7.IFD Analysis of the hits compounds

Hits	Glide Energy	Glide Emodel	Docking Score	Ifdscore	Interaction par liaison hydrogène	Interaction Hydrophobe	Interaction Pi-Pi ,Pi-Cation,Salt Bridge
Z1804044680	-57.589	-92.654	-12.718	-982.873	His259,val435	, Tyr76, Phe78, Met79, Phe83, Leu100, Phe255, Ala256, Leu321, Met433, Val434	Tyr76[a], phe78[a,b], hem460[b]
PV-001850708261	-52.992	-76.704	-10.799	-983.980	Thr260, gln72	Tyr76, Phe78, Met79, Phe255, Leu321	Hem460[a], tyr76[a]
Z2283404606	-61.114	-108.122	-13.504	-982.746	val435 , his259	Tyr76, Phe78, Met79, Phe83, Met99, Leu100, Phe255, Ala256, Leu321, Val434	Phe78[a],tyr76[a]
Z1651668373	-62.123	-96.840	-12.442	-982.017	Thr260, his259	Tyr76, Phe78, Met79, Phe83, Leu100, Phe255, Ala256, Leu321	Hem460[b,c], phe78[a]
PV-001935350830	-60.930	-100.715	-11.685	-981.866	Ile323, pro320,val435	Tyr76, Phe78, Met79, Phe83, Phe255, Ala256, Leu321, Val434,	Phe78[a], hem460[a]
PV-001831793679	-61.382	-108.534	-12.787	-981.467	His259, ile323, val435	Tyr76, Phe78, Met79, Phe83, Leu100, Phe255, Leu321, Ile322, Ile323, Met433, Val434	Phe78[a], Tyr76[a]
PV-001862316134	-60.603	-98.435	-12.384	-981.223	Ala256, thr260	Tyr76, Phe78, Met79, Met99, Leu100, Phe255, Ala256, Leu321	Hem460[a,b]
PV-001924736320	-62.682	-99.808	-13.786	-981.078	Arg95, ser252	Tyr76, Phe78, Met79, , Met99, Leu100, Phe255, Ala256, Leu321	Phe83[a], phe78[a],hem460[b,c]
Z1545254023	-51.409	-87.496	-11.648	-980.913	His259, thr260, val435	Tyr76, Phe78, Met79, Phe83, Phe255, Ala256, , Leu321, Ile323, Val434	Phe78[a], Tyr76[a,b] Hem460[b,c]
PV-001925585102	-52.422	-87.198	-12.085	-980.654	His259, val435	Tyr76, Phe78, Met79, Phe83, Met99, Leu100, Phe255, Ala256, Leu321, ,Val434	Phe78[a], Tyr76[a,b] Hem460[b]
Z2141883735	-55.633	-90.514	-11.834	-980.457	His259, thr260, val435	Tyr76, Phe78, Met79, Phe255, Ala256, , Leu321, Val434	Phe78[a], Tyr76[a] Hem460[a]

PV-001921223059	-58.625	-91.232	-13.259	-980.317	His259, thr260	Tyr76, Phe78, Met79, Phe83, Leu100, Ala256, Leu321, Ile323, Met433, Val434,Leu324	Phe78[a], Tyr76[a] Arg96[b],Hem460[b,c]
Z2770976320	-58.503	-96.359	-11.560	-980.065	Ser252,val435,his259	Tyr76, Phe78, Met79, Phe83, , Met99, Leu100, Phe255, Leu321	Phe78[a]
Z2903058602	-56.000	-80.798	-11.551	-979.947	His259, val435	Tyr76, Phe78, Met99, Leu100, Leu321, Ile323, Met433, Val434	Tyr76[a],phe78[a],phe83[a]
Z2193901479	-54.583	-90.923	-10.680	-979.841	Thr260,ala256	Tyr76, Phe78, Met79, Phe83, Met99, Leu100, Phe255, Ala256, Leu321, Val434	Hem460[a,b]
Z2218766564	-60.258	-104.094	-11.573	-979.509	Arg95,His259,thr260	Tyr76, Phe78, Met79, Phe83, Leu100, Phe255, Ala256, Leu321, Val434	Phe78[a] ,Hem460[b]
Z2903057141	-44.602	-75.456	-10.229	-979.264	Met433	Tyr76, Phe78, Met79, Phe83,Met99, Leu100, Phe255, Ala256, Leu321, Ile322, Ile323	Phe78, hem460
PV-000817165047	-60.296	-94.087	-11.762	-978.162	Val435	Tyr76, Phe78, Phe255, Leu321, Ile323, Met325	Phe78[a], hem460[a,c]
Z2095183789	-63.187	-112.728	-13.066	-985.918	Val435	Gln72, Tyr76, Phe78, Met79, Phe83, Arg95, Arg96, Met99, Leu100, Phe255, Ala256, His259, Thr260, Leu321, Ile322, Ile323, Met325 Met433, Val434,Leu324	Phe78[a], hem460[a,c]
Z3188961853	-56.528	-97.253	-11.305	-978.450	Met433	Tyr76, Phe78, Met79, Phe83, Met99, Leu100, Phe255, Ala256, Leu321, Ile323, Met433, Val434	Tyr76[a], phe78[a]
Z2923423811	-62.538	-106.940	-14.041	-983.891	Ile323,his259,val435	Tyr76, Phe78, Met79, Met99, Leu100, Phe255, Ala256, Leu321, Val434	Phe78[a]
PV-002587460686	-60.672	-100.510	-11.723	-983.860	Arg95, arg96, hem460, his259	Tyr76, Phe78, Met79, Phe83, Phe255, Ala256, Leu321, Ile323, Met325 Met433	Tyr76[a], hem460[a]
PV-001936869335	-58.959	-95.643	-11.608	-981.634	Met433,arg95,ser252	Tyr76, Phe78, Met79, Phe83, Met99, Leu100, ser252 Phe255,	Phe78[a], hem460[a]

						Ala256, Leu321, Val434	
Z1498805014	-61.361	-99.213	-12.218	-980.572	Arg95, met433	Tyr76, Phe78, Met79, Phe83, Leu100, Phe255, Ala256, Leu321, Ile323, Val434	Hem460[b,c]
Z1849714935	-58.599	-95.006	-11.390	-979.448	His259, thr260	Tyr76, Phe78, Met79, Phe83, Met99, Leu100, Phe255, Leu321, Val434	Phe78, hem460[b,c]
Z1753455598	-59.452	-91.648	-11.862	-976.845	Thr260	Tyr76, Phe78, Met79, Phe83, Met99, Leu100, Phe255, Leu321, Val434	Phe78[a], Arg95[b], Hem460[b]
FLUCONAZOLE	-49.029	-72.175	-7.158	-977.380	His259,thr260	Tyr76, Phe78, Met79, Phe83,Phe255, Leu321	Hem460[a]

a : pi-pi interaction

b :pi-cation interaction

c :interaction salt bridge

- 🔴 Charged (negative)
- 🟣 Charged (positive)
- Glycine
- Hydrophobic
- Metal
- 🔵 Polar
- ⚫ Unspecified residue
- ⚪ Water
- Hydration site
- ✖ Hydration site (displaced)
- ┄┄ Distance
- ➤ H-bond
- ─── Metal coordination
- ●━● Pi-Pi stacking
- ●━● Pi-cation
- ─── Salt bridge
- Solvent exposure
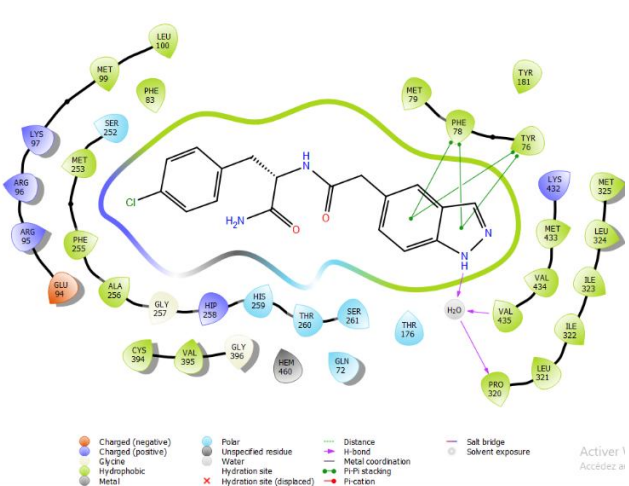
Z2095183789
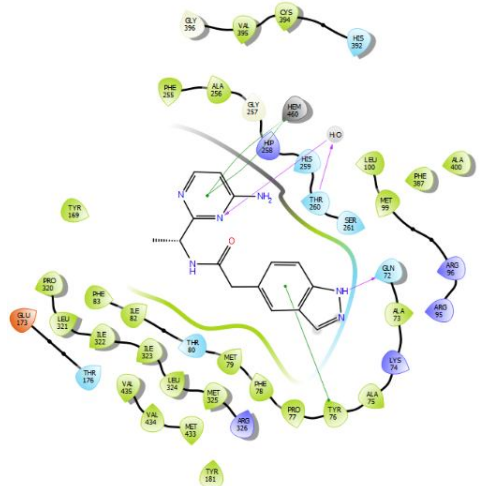
PV-001850708261
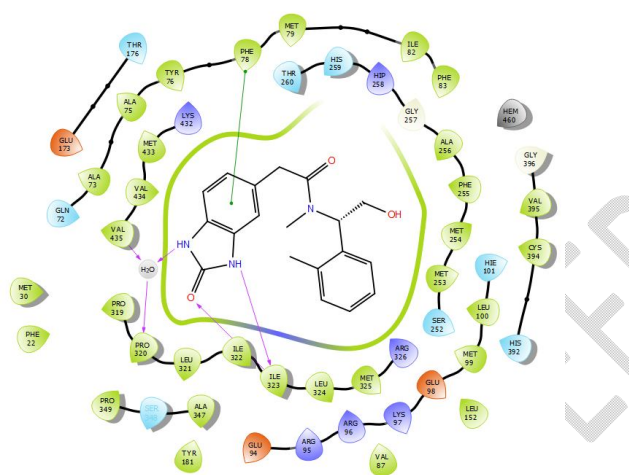
Z2923423811
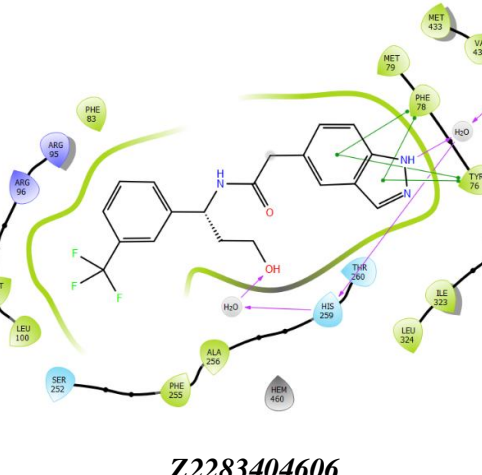
Z2283404606
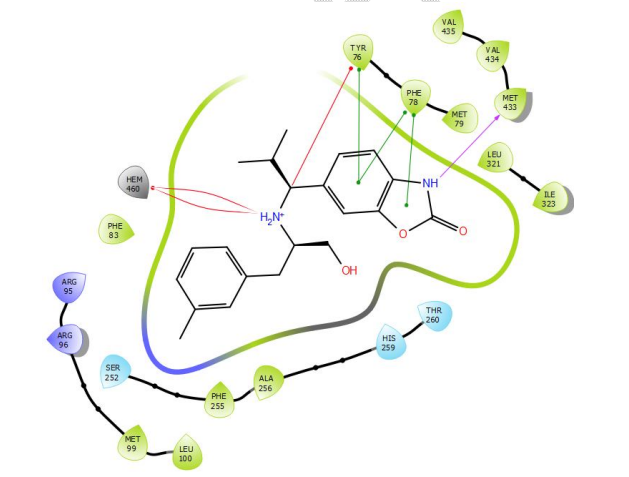
Z1804044680
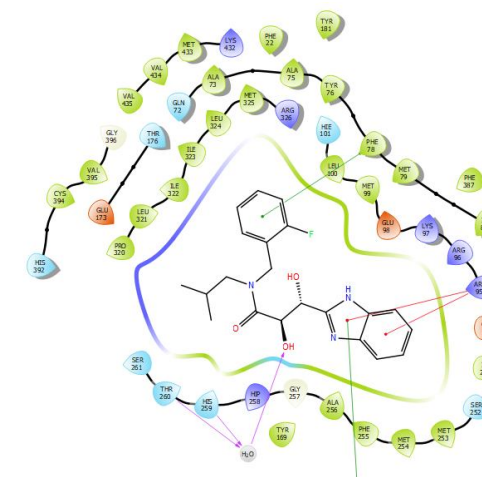
Z1753455598

Figure 3: Interactions of hits with the lowest IFD scores.

Figure IV.4 illustrates the interactions of the HITS **Z2283404606**, **Z1804044680**, **Z2923423811**, **PV-001850708261**, **Z2095183789** which have the lowest IFDscore as well as the lead Z1753455598 which has the highest IFDscore with residues of the candida albicans active site. The binding modes of the leads with the lowest IFDscore (**Z2923423811**, **PV-001850708261**, **Z2095183789**) as well as the one with the highest IFDscore (**Z1753455598**) were discussed in detail.

- **Binding mode of Z2095183789**

The lead **Z2095183789** has an IFDscore of -985.918kcal/mol and a considerably low docking score of -13.066kcal/mol, which is lower than that of the standard co-crystallised ligand (IFDscore= -977.380kcal/mol ; Dockingcore= -7.158 kcal/mol). The lead **Z2095183789** binds to the 1EA1 receptor active site by forming four hydrogen bonds, a direct hydrogen bond with residue Met433 and hydrogen bonds via a water molecule with residues Val435, Pro320 and His259 of the active site (Figure IV.5 and IV.6). The first hydrogen bond is established between the oxygen of the carbonyl group c=o of residue Met433 and a hydrogen atom of the 2-pyrazoline heterocycle of the ligand with the parameters ($d(H \cdots Y) = 1.90$ Å ; $d(X \cdots Y) = 2.83$; Å $\angle XHY = 151.6°$).
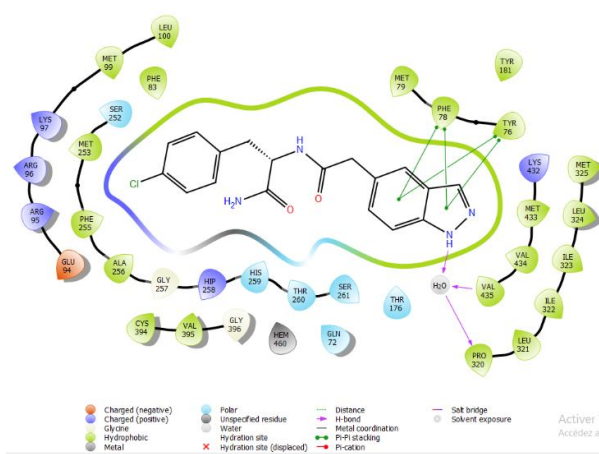
Figure4 : Binding mode of the hitZ2095183789
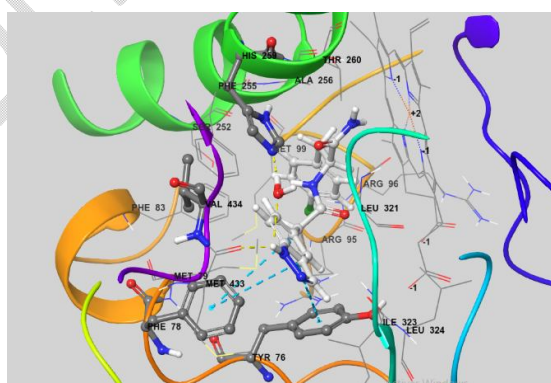
Fig.5.3D binding mode of the hit Z2095183789 in the active site of 1EA1(hydrogen bonding:yellow colour;pi-pi interaction:blue colour
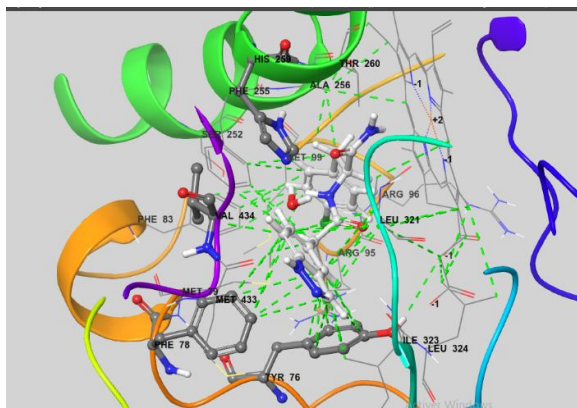
Fig.6. Hydrophobic interactions of the hit Z2095183789 with the active site residues of 1EA1.

Three hydrogen bonds are formed between a hydrogen atom of the pyrazoline ring and residues Val435, Pro320 and His259 via a water molecule with the following hydrogen bond parameters (ligand-H$_2$O : $d(H \cdots Y)$=2.63 Å, $d(X \cdots Y)$=3 .29 Å $\angle XHY$=123.3 ;H$_2$O-Val435 : $d(H \cdots Y)$=1.93 Å ,$d(X \cdots Y)$=2.93 Å $\angle XHY$=169.2° ; H$_2$O-Pro320 : $d(H \cdots Y)$=1.71Å ,$d(X \cdots Y)$=2.72 Å $\angle XHY$=173.7° H$_2$O-His259 : $d(H \cdots Y)$=1.80 Å ,$d(X \cdots Y)$=2.80 Å $\angle XHY$=174.7°).

Furthermore we found that the indazole ring establishes two pi-pi bonds with residues Tyr76 and Phe78. In addition the compound Z2095183789 shows hydrophobic interactions with residues Tyr76, Phe78, Met79, Phe83, Met99, Phe255, Ala256, Leu321, Ile323, Val434, (Figure 7) which allows the fixation of the ligand in the active site of the enzyme.

Also we presented in Figure .8 another pose of the lead Z2095183789 ((IFDscore= -984.728 kcal/mol ; Dockingscore= -12.435 kcal/mol) in order to highlight the possibility of the latter to form hydrogen bonds with residues Thr260 and His259 of the active site like fluconazole.
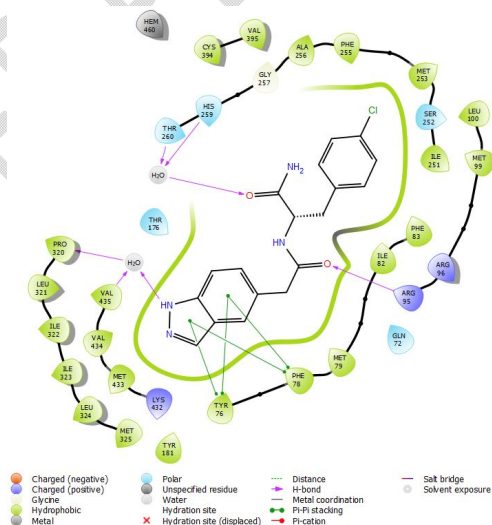
Fig.7.Binding mode of the lead Z2095183789 with interaction with Thr260 and His259

- **Binding mode ofPV-001850708261**

The molecule *PV-001850708261* has an **IFDscore** and a **docking score** of **-10.799 kcal/mol**, which is lower than that of the co-crystallized ligand. It forms two hydrogen bonds with the residues **Gln72**

and **Thr260** in the active site of receptor **1EA1** (Figures 9 and 10), with the following geometric parameters: **Gln72** ($d(H \cdots Y)$=2.06 Å , $d(X \cdots Y)$=3,00Å ∠XHY=153.10°) ; **Thr260** (**ligand-H2O**: $d(H \cdots Y) = 2.16$Å , $d(X \cdots Y) = 3.17$ Å ∠$XHY = 171.40°$ **H2O − Thr260**: $d(H \cdots Y) = 1.92$ Å ; $d(X \cdots Y) = 2.93$ Å ; ∠$XHY = 178.3°$).

Furthermore, the molecule PV-001850708261 interacts with residues **Tyr76** and **Hem460** through **pi-pi** and **pi-cation** interactions, respectively. Additionally, PV-001850708261 forms hydrophobic interactions with**Tyr76**, **Phe78**, **Met79**, **Phe255**, and **Leu321** in the active site of the protein (Fig.11).
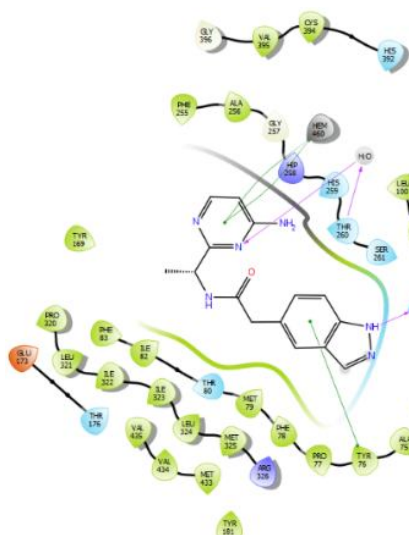
Figure.8: Binding mode of the hit PV-001850708261
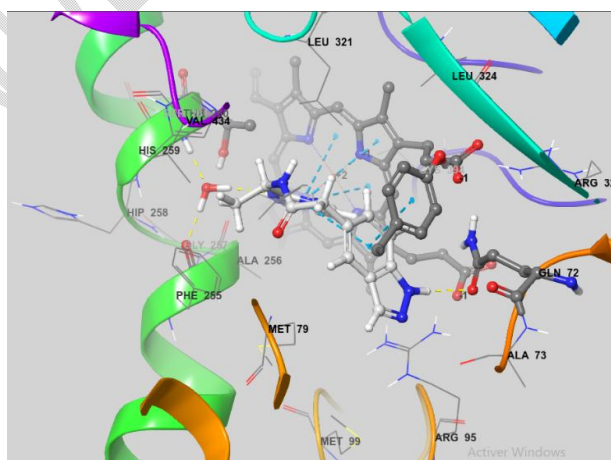
Figure 9: Binding mode of the hit PV-001850708261 in the active site of 1EA1
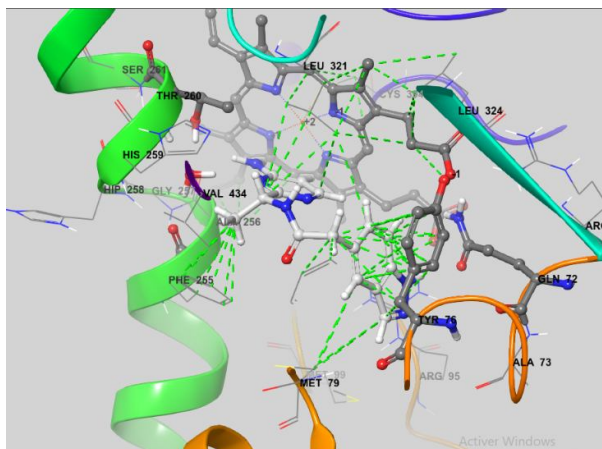
Fig.11. Hydrophobic interactions of the hit PV-001850708261 with the residues in the active site of 1EA1

- **Binding mode of Z2923423811**

Z2923423811 has an IFDscore of -983.891kcal/mol and a Docking score of -11.723kcal/mol, lower than that of fluconazole. It binds to the active site of the protein target by forming four hydrogen bonds with residues Ile323, His259, Val435, Pro320 and a pi-pi interaction with residue Phe78 (Figure VI.12 and VI.13). The geometric parameters of the different hydrogen bonds are as follows:**Ile322** (d(H⋯Y)=2.15 Å ,d(X⋯Y)=3.15Å   ∠XHY=167°) ;**Ile323** (d(H⋯Y)=1.88 Å ,d(X⋯Y)=3.00Å ∠XHY=153.10°);

Val435, Pro320 (ligand-H2O:d(H⋯Y) = 2.12Å ,d(X⋯Y) = 2.98 Å ∠XHY = 141.70°

H2O − Pro320: d(H⋯Y) = 1.71 Å ; d(X⋯Y) = 2.72 Å ; ∠XHY = 175.6°.

H2O − Val435: $d(H ⋯ Y)$ = 1.87 Å ; $d(X ⋯ Y)$ = 2.86 Å ; ∠XHY = 162.7).
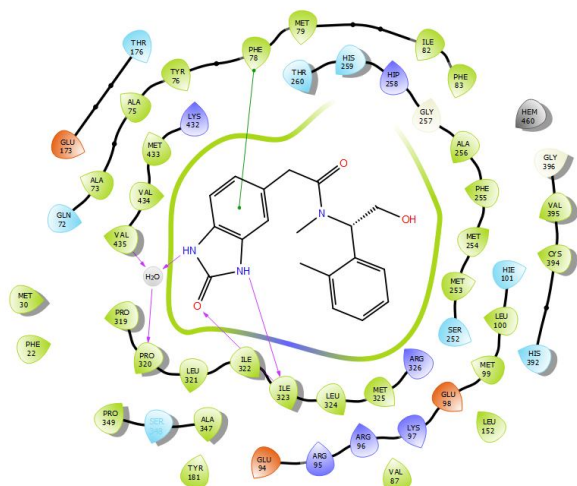
Fig.10.Binding mode of the hitZ2923423811
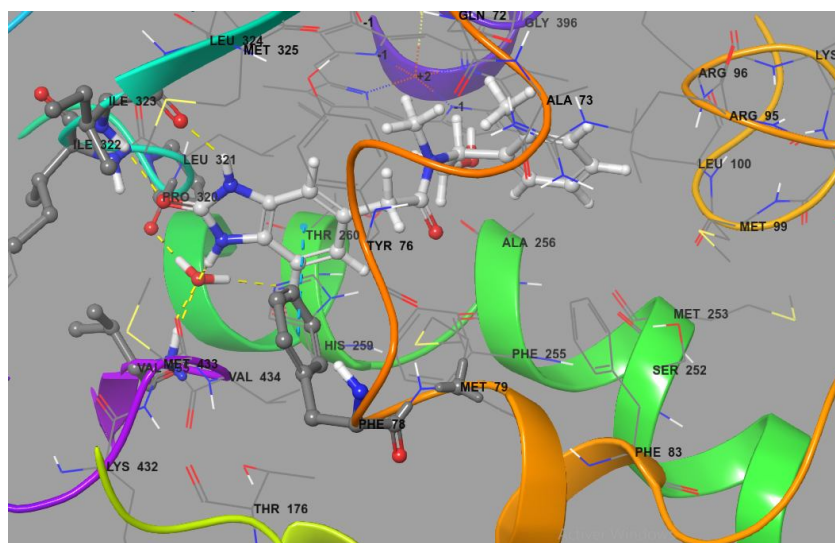
Fig.11. 3D binding mode of the hit Z2923423811 in the active site of 1EA1

Furthermore, the molecule Z2923423811 forms hydrophobic interactions with the residues **Tyr76**, **Phe78**, **Met79**, **Met99**, **Leu100**, **Phe255**, **Ala256**, **Leu321**, and **Val434** in the active site (Figure 14).
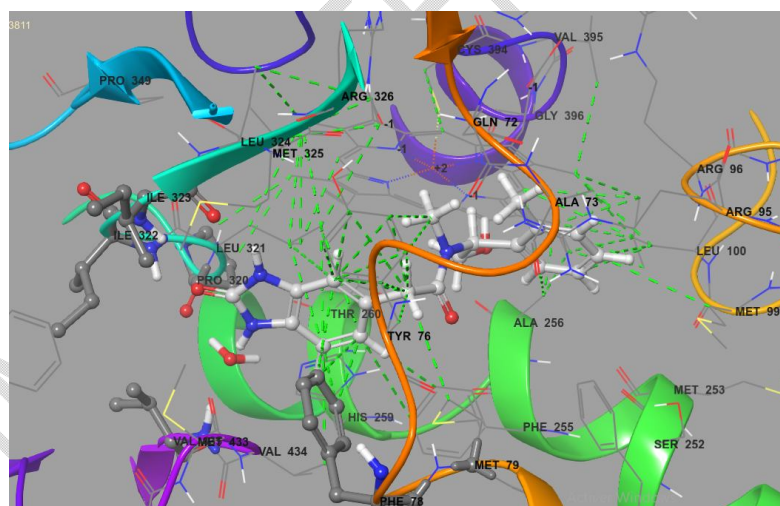
Fig.12. Hydrophobic interactions of the hit Z2923423811 with the residues in the active site of 1EA1

- **Mode de liaison de *Z1753455598***

Regarding the molecule **Z1753455598**, it has the highest IFDscore among the identified molecules. This parameter is slightly higher than that of the co-crystallized ligand (Fluconazole: IFDScore = -977.380 kcal/mol; Docking Score = -7.158 kcal/mol).**Z1753455598** binds to the active site by forming two hydrogen bonds with residues Thr260 and His259 through a water molecule (Figures VI.15 and VI.16) with the following geometric parameters:

Ligand-H2O:$d(H \cdots Y) = 1.88$Å $, d(X \cdots Y) = 2.87$ Å $\angle XHY = 167.90°$

H2O − **His259** : $d(H \cdots Y) = 1.62$ Å $; d(X \cdots Y) = 2.64$ Å $; \angle XHY = 166.7°$

H2O − **Thr260**: $d(H \cdots Y) = 2.22$ Å $; d(X \cdots Y) = 3.23$ Å $; \angle XHY = 171°$),

The molecule Z1753455598 also forms pi-cation interactions with residue Arg95 and pi-pi interactions with residue Phe78 and the heme molecule (HEM450) in the active site.The visualization of the 3D docking pose (Figure VI.17) shows that compound Z1753455598 establishes several hydrophobic interactions with active site residues, including Tyr76, Phe78, Met79, Phe83, Met99, Leu100, Phe255, Leu321, and Val434.
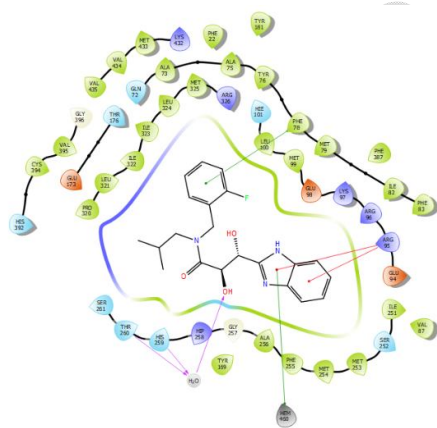
Fig.13.Binding mode of the hit Z1753455598.
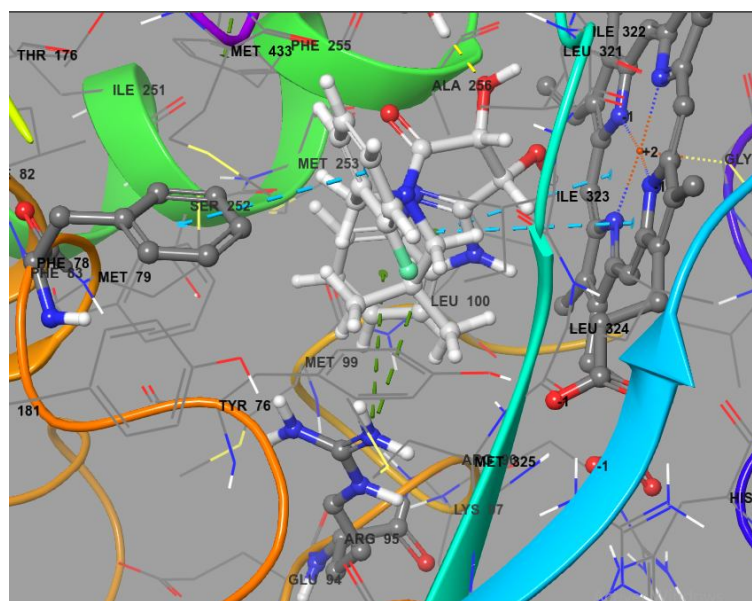
Fig.14.3D binding mode of the molecule Z1753455598 in the active site of 1EA1
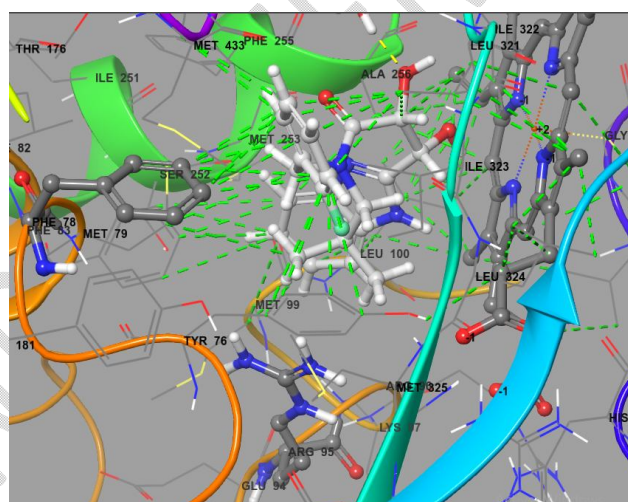
Fig.15. Hydrophobic interactions of the molecule Z1753455598 with the residues in the active site of 1EA1

Except for the molecule Z2723048448, all ligands have **IFDscore** and **Docking score** parameters lower than those of fluconazole. Similarly, the docking pose analysis of the molecules revealed that they form hydrogen bonds, **pi-pi**, **pi-cation**, and hydrophobic interactions with the residues of the active site, similar to those of the reference ligand. The predominant protein-ligand interactions in the different poses are the hydrophobic interactions. Other molecules exhibit additional hydrogen bonds. The binding mode via **IFD** presented above shows that these different molecules are strong

candidates for the inhibition of *Candida albicans* and could be further optimized to improve their activity profile.

3.7 Prediction of ADMET parameters

The ADME properties of the 26 newly identified molecules were evaluated using Qikprop. The results are summarized in Table VI.8. The 26 molecules mentioned above comply with the drug-like properties based on Lipinski's Rule of Five. The pharmacokinetic parameters (ADME-Tox) for the 26 molecules were found to fall within an acceptable range for human use, revealing their potential drug-like properties.

Table 8: ADME properties of the hits

Hits	MW	donor HB	Accpt HB	QPlogw	QPlogPo/w	QPlogS	QPPCaco	Human Oral Absorption	Percent Human Oral Absorption
Z1753455598	385.437	2.000	6.900	13.314	3.131	-3.952	851.982	3	100.000
Z1849714935	353.438	3.000	5.200	11.570	2.665	-1.560	119.567	3	79.735
Z1498805014	388.413	3.000	6.150	13.250	3.204	-3.883	209.810	3	87.261
PV-001936869335	412.450	3.000	9.200	15.425	1.110	-2.698	115.007	3	70.329
PV-001935350830	375.374	2.000	7.500	13.696	1.655	-3.712	155.446	3	75.859
PV-001831793679	391.512	3.000	5.700	12.761	4.118	-6.087	575.988	3	100.000
PV-001850708261	296.331	4.000	6.000	17.195	0.858	-2.555	89.151	3	66.870
Z1651668373	342.430	3.000	4.000	13.276	3.103	-2.771	219.261	3	87.014
Z2283404606	377.365	3.000	5.700	14.544	2.268	-2.862	205.131	3	81.607
Z1804044680	354.448	3.000	6.200	12.316	2.480	-3.007	112.569	3	78.182
Z2141883735	340.378	1.000	6.750	10.553	2.811	-4.288	672.074	3	94.009
PV-001924736320	323.412	3.000	4.200	11.768	2.907	-3.436	190.101	3	84.754
Z1545254023	299.347	3.000	4.700	11.530	2.372	-2.810	161.927	3	80.374
PV-001921223059	390.308	3.000	4.900	10.808	3.211	-2.292	323.035	3	90.657
PV-001925585102	350.340	3.000	3.200	9.652	3.295	-2.640	361.479	3	92.024
Z2095183789	356.811	3.250	5.250	17.535	1.093	-1.124	47.951	2	63.427
PV-002587460686	365.431	4.250	5.000	16.937	2.322	-3.894	67.392	2	73.268
PV-000817165047	348.447	3.000	5.000	12.170	3.465	-3.862	285.062	3	91.174
Z2923423811	339.393	3.000	6.700	14.844	1.493	-3.830	141.444	3	74.177
Z2770976320	368.333	2.000	6.250	11.894	2.457	-4.840	314.070	3	86.023
Z2903058602	355.300	1.000	5.500	11.104	3.234	-5.040	789.469	3	100.000
Z2218766564	359.372	2.000	5.900	10.985	2.486	-2.339	282.022	3	85.356
Z2193901479	325.301	1.000	6.250	10.851	2.255	-4.328	311.617	3	84.781
Z3188961853	351.450	2.000	5.000	11.613	2.714	-2.111	313.274	3	87.511
PV-001862316134	351.401	3.000	4.700	12.156	3.515	-4.812	377.819	3	93.655
Z2903057141	309.281	1.000	6.750	11.834	1.714	-3.386	674.823	3	87.618

MW Molecular Weight (Acceptable range: MW < 500).

DonorHB : Estimation of the number of hydrogen bonds that the ligand can donate (Marge acceptable : 0,0 - 6,0).

AccptHB : Estimation of the number of hydrogen bonds a ligand can accept (Marge acceptable : 2,0 - 20,0).

QPlogPw: Predicted water/gas partition coefficient (Marge acceptable: 4,0 - 45 ,0).

QPlogP0/w: Predicted octanol/water partition coefficient (Marge acceptable : -2,0 – 6,5).

QPlogS: Predicted aqueous solubility, logarithm in mol dm–3 (Marge acceptable : -6,5 – 0,5)
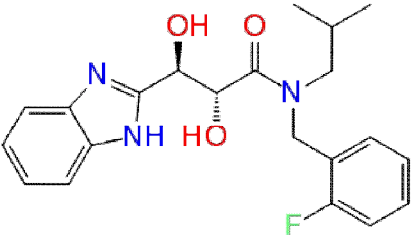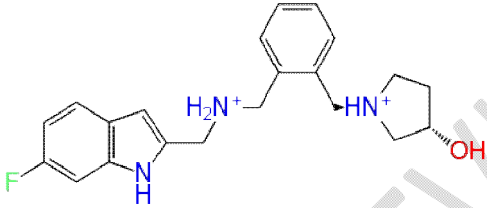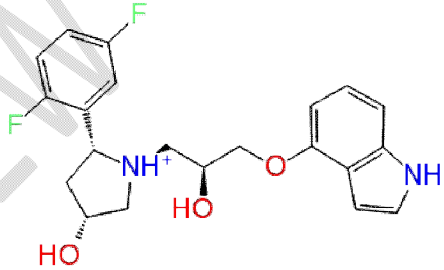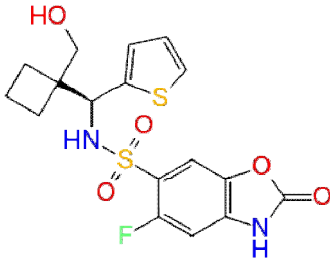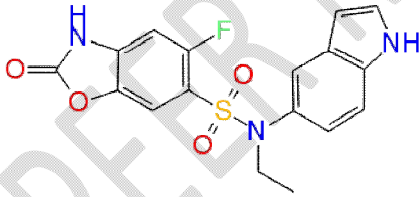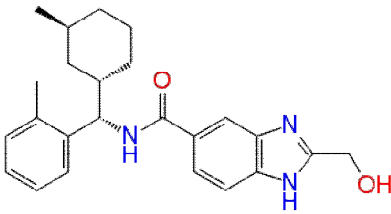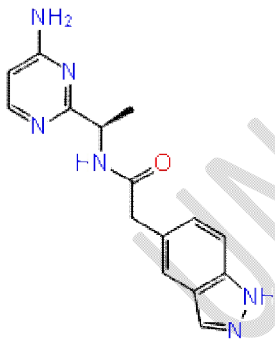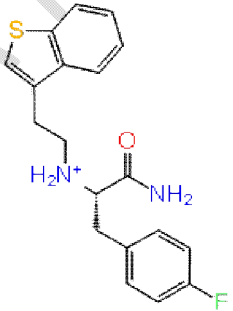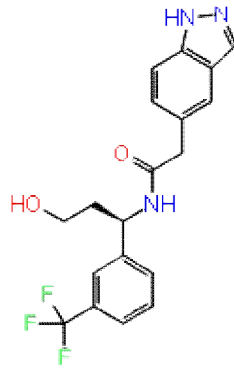
QPPCaco: Predicted apparent Caco-2 cell permeability in nm/sec (< 25 : low et >500 : high).
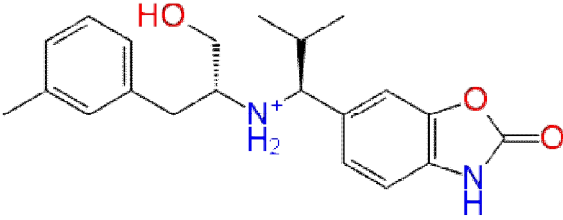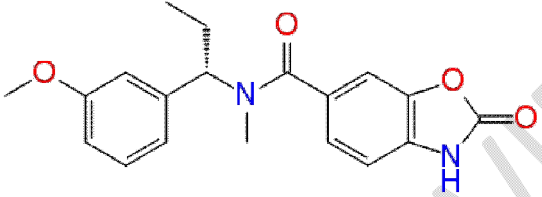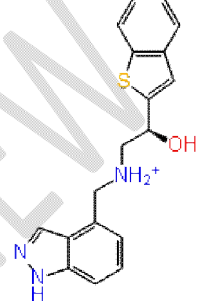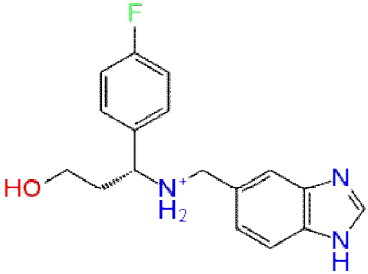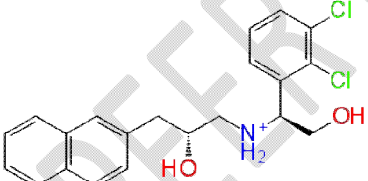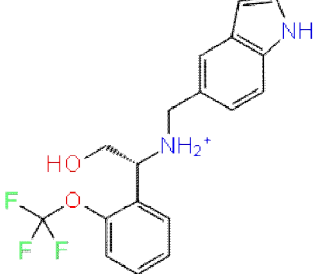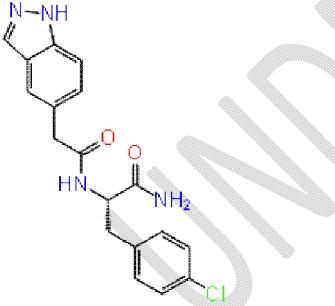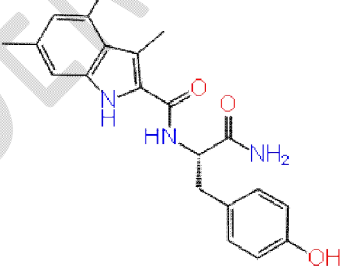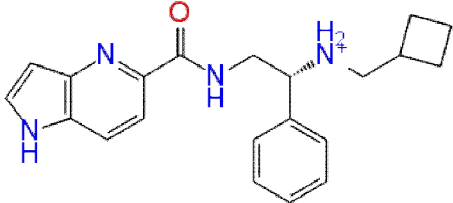
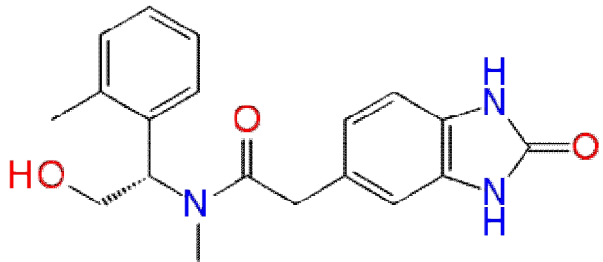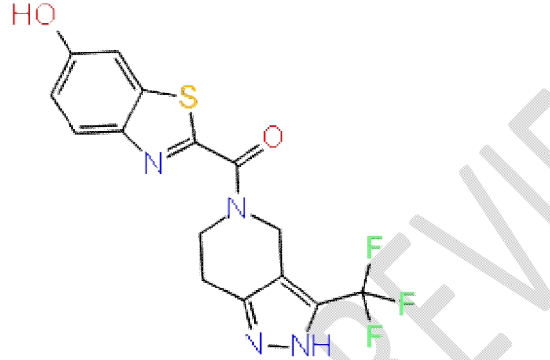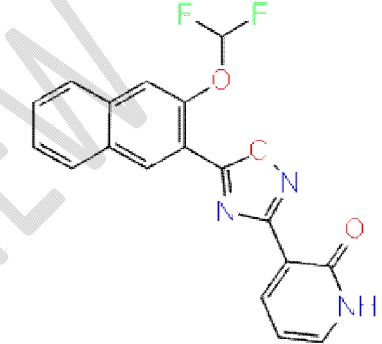PHOA : Human Oral Absorption Percentage (80% is high, and 25% is low)
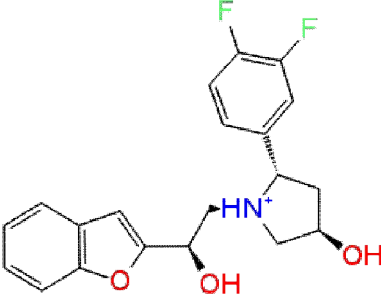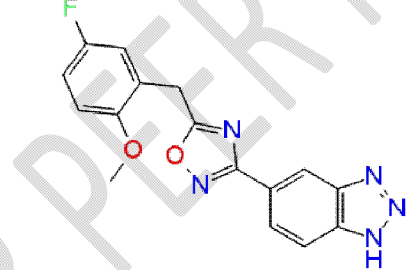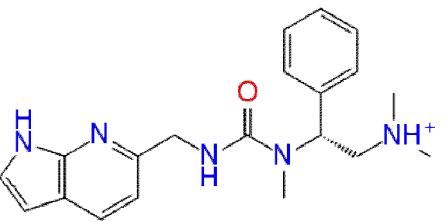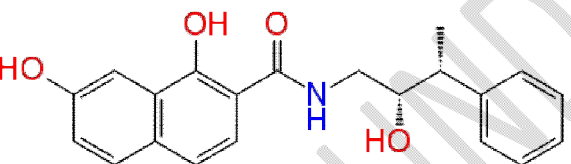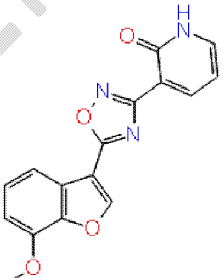
HOA : Predicted Oral Absorption on a scale from 1 to 3. (1: Low absorption, 2: Moderate absorption, 3: High absorption)

Table.9: 2D structures of the obtained hits.

Z1753455598

Z1849714935

Z1498805014

PV-001936869335

PV-001935350830

PV-001831793679

PV-001850708261

Z1651668373

Z2283404606

Z1804044680

Z2141883735

PV-001924736320

Z1545254023

PV-001921223059

PV-001925585102

Z2095183789

PV-002587460686

PV-000817165047

Z2923423811

Z2770976320

Z2903058602

Z2218766564

Z2193901479

Z3188961853

PV-001862316134

Z2903057141

Conclusion

A virtual screening procedure based on pharmacophore models derived from a set of antifungal molecules and the crystal structure of Candida albicans was applied to a compound library (Enamine) to identify new potential inhibitors of Candida albicans. Firstly, the Enamine database was filtered and processed to target only "drug-like" molecules. The selected set of molecules was then docked into the active site of Candida albicans (PDB ID: 1EA1) to assess and gain an in-depth understanding of their binding capability within the enzyme's active site.

Docking analysis revealed that the 26 identified hits interact with the active site residues in a manner similar to the reference inhibitor, fluconazole. These interactions include hydrogen bonds, pi-pi, pi-cation, and hydrophobic interactions. The predominant interactions are mainly observed with residues His259, Thr260, Phe78, Tyr76, and Hem460. Finally, an ADME study was performed for the 26 hits to assess their toxicity and pharmacokinetic properties. The analysis of the results shows that these molecules exhibit pharmacokinetic parameter values within the acceptable range for human use. The findings of this study may provide insights into the development of new potent inhibitors of Candida albicans.

Further studies will be necessary to better understand the stability of the hits over time within the active site of enzyme 1EA1 through molecular dynamics simulations. The molecules retained after this study will be proposed for organic synthesis and biological testing.

References

1. Di Santo R (2010) Natural products as antifungal agents against clinically relevant pathogens. Nat Prod Rep 27:1084–1098. https://doi.org/10.1039/b914961a
2. Vázquez-González D, Perusquía-Ortiz AM, Hundeiker M et al. (2013) Opportunistic yeast infections: candidiasis, cryptococcosis, trichosporonosis and geotrichosis. J Dtsch Dermatol Ges 11:381-93; quiz 394. https://doi.org/10.1111/ddg.12097
3. Wächtler B, Citiulo F, Jablonowski N et al. (2012) Candida albicans-epithelial interactions: dissecting the roles of active penetration, induced endocytosis and host factors on the infection process. PLoS ONE 7:e36952. https://doi.org/10.1371/journal.pone.0036952
4. Schiaffella F, Macchiarulo A, Milanese L et al. (2005) Design, synthesis, and microbiological evaluation of new Candida albicans CYP51 inhibitors. Journal of medicinal chemistry 48:7658–7666. https://doi.org/10.1021/jm050685j
5. Sheehan DJ, Hitchcock CA, Sibley CM (1999) Current and Emerging Azole Antifungal Agents. Clin Microbiol Rev 12:40–79
6. Chimenti F, Bizzarri B, Maccioni E et al. (2007) Synthesis and in vitro activity of 2-thiazolylhydrazone derivatives compared with the activity of clotrimazole against clinical isolates of Candida spp. Bioorganic & Medicinal Chemistry Letters 17:4635–4640. https://doi.org/10.1016/j.bmcl.2007.05.078
7. Podust LM, Poulos TL, Waterman MR (2001) Crystal structure of cytochrome P450 14alpha -sterol demethylase (CYP51) from Mycobacterium tuberculosis in complex with azole inhibitors. Proc Natl Acad Sci U S A 98:3068–3073. https://doi.org/10.1073/pnas.061562898
8. Sagatova AA, Keniya MV, Wilson RK et al. (2015) Structural Insights into Binding of the Antifungal Drug Fluconazole to Saccharomyces cerevisiae Lanosterol 14α-Demethylase. Antimicrob Agents Chemother 59:4982–4989. https://doi.org/10.1128/AAC.00925-15
9. Luca L de (2006) Naturally occurring and synthetic imidazoles: their chemistry and their biological activities. Curr Med Chem 13:1–23
10. Zhu J, Lu J, Zhou Y et al. (2006) Design, synthesis, and antifungal activities in vitro of novel tetrahydroisoquinoline compounds based on the structure of lanosterol 14alpha-demethylase (CYP51) of fungi. Bioorganic & Medicinal Chemistry Letters 16:5285–5289. https://doi.org/10.1016/j.bmcl.2006.08.001
11. Roberts TR, Hutson DH, Lee PW et al. (2007) Metabolic Pathways of Agrochemicals. Royal Society of Chemistry, Cambridge
12. D. Zon, A. Kone, M. Ouattara Synthèse et Activités Antifongiques de Nouveaux Benzimidazoles à Fonction 2-Arylacrylonitrile Ou 2- Cyanoarylpropénone. Rev Ivo Ir Ci Technol 2014 3:41–53
13. Drissa Sissouma, Mahama. Ouattara, Doumade Zon (2015) Synthesis and Antifungal Activities of Some Benzimidazolyl-Chalcones, Analogues of Chlormidazole. Afr. J. Pharm. Pharmacol. 9 (12):418–423
14. Schrödinger Release 2017-4: LigPrep, Schrödinger, LLC, New York, NY, 2017.
15. Shivakumar D, Williams J, Wu Y et al. (2010) Prediction of absolute solvation free energies using molecular dynamics free energy perturbation and the OPLS force field. Journal of chemical theory and computation 6:1509–1519

16. Dixon SL, Smondyrev AM, Knoll EH et al. (2006) PHASE: A new engine for pharmacophore perception, 3D QSAR model development, and 3D database screening: 1. Methodology and preliminary results. Journal of computer-aided molecular design 20:647–671

17. Dixon SL, Smondyrev AM, Rao SN (2006) PHASE: A novel approach to pharmacophore modeling and 3D database searching. Chemical biology & drug design 67:370–372

18. Huang N, Shoichet BK, Irwin JJ (2006) Benchmarking sets for molecular docking. Journal of medicinal chemistry 49:6789–6801

19. Mysinger MM, Carchia M, Irwin JJ et al. (2012) Directory of useful decoys, enhanced (DUD-E): Better ligands and decoys for better benchmarking. Journal of medicinal chemistry 55:6582–6594

20. Schrödinger Release 2017-4: Phase, Schrödinger, LLC, New York, NY, 2017.

21. Braga RC, Andrade CH (2013) Assessing the performance of 3D pharmacophore models in virtual screening: How good are they? Current topics in medicinal chemistry 13:1127–1138

22. J. M. Yang and T. W. Shen, "A pharmacophorebased evolutionary approach for screening selective

23. Wang H, Aslanian R, Madison VS (2008) Induced-fit docking of mometasone furoate and further evidence for glucocorticoid receptor 17α pocket flexibility. Journal of Molecular Graphics and Modelling 27:512–521

24. Saubern S, Guha R, Baell JB (2011) KNIME workflow to assess PAINS filters in SMARTS format. Comparison of RDKit and Indigo cheminformatics libraries. Molecular Informatics 30:847–850

25. Schrödinger Release 2019-4: QikProp, Schrödinger, LLC, New York, NY, 2017.

26. Dixon SL, Smondyrev AM, Knoll EH et al. (2006) PHASE: a new engine for pharmacophore perception, 3D QSAR model development, and 3D database screening: 1. Methodology and preliminary results. Journal of computer-aided molecular design 20:647–671. https://doi.org/10.1007/s10822-006-9087-6

27. Truchon J-F, Bayly CI (2007) Evaluating virtual screening methods: good and bad metrics for the "early recognition" problem. J Chem Inf Model 47:488–508. https://doi.org/10.1021/ci600426e

28. Patel S, Modi P, Chhabria M (2018) Rational approach to identify newer caspase-1 inhibitors using pharmacophore based virtual screening, docking and molecular dynamic simulation studies. Journal of Molecular Graphics and Modelling 81:106–115. https://doi.org/10.1016/j.jmgm.2018.02.017